

X rays from foil-excited iodine beams*

C. L. Cocke, S. L. Varghese, J. A. Bednar,[†] C. P. Bhalla, B. Curnutte,
R. Kauffman,[‡] R. Randall,[§] P. Richard, and C. Woods^{||}
Department of Physics, Kansas State University, Manhattan, Kansas 66506

J. H. Scofield

Lawrence Livermore Laboratory, Livermore, California 94550

(Received 16 June 1975)

M-x-ray spectra from foil-excited iodine beams between 40 and 62 MeV have been studied using a bent-crystal spectrometer. The prompt spectrum is so rich as to defy analysis, but the delayed spectrum exhibits a number of resolved lines. Electric quadrupole $4s \rightarrow 3d$ transitions are observed from metastable systems in the NiI, CuI, and ZnI isoelectronic sequences. Electric dipole $4p \rightarrow 3d$ transitions from states in these isoelectronic sequences also appear downstream. Transition energies and quadrupole lifetimes have been measured and are compared with the results of both relativistic and nonrelativistic calculations.

I. INTRODUCTION

A recent revival of interest in the x-ray spectroscopy of very highly ionized systems has stemmed from the importance of such x rays both as a source of energy loss from and as a possible diagnostic tool for the analysis of very-high-temperature plasmas. Such plasmas are encountered, for example, in controlled-thermonuclear-reaction (CTR) devices and from the interaction of high-power lasers with matter. There exist large gaps in analyses of multiply ionized systems, gaps which are filled to a limited extent by spectroscopy on high-temperature laboratory plasmas. Here we explore the usefulness of the beam-foil source for the study of x-ray spectra from highly ionized iodine.

Foil-excited beams in the MeV/amu range have long been known to represent high "equivalent-temperature" sources. Because allowed x-ray decays take place very near the foil, the source is particularly well suited for study of both energies and lifetimes of metastable systems by the observation of x rays downstream. This characteristic is to be contrasted to that of hot-plasma radiation sources which generally display primarily the strong-allowed decays. This paper reports the use of foil-excited beams of iodine to study *M* x-ray spectra in the NiI, CuI, and ZnI isoelectronic series for $Z = 53$. While the major emphasis is on the study of long-lived systems whose decay is electric quadrupole, electric-dipole decays have been observed as well and are discussed.

The NiI isoelectronic sequence represents a particularly attractive case for the study of metastable states possessing energetic vacancies. Since the ground-state configuration, for Z greater than 28, is that of a closed *M* shell, low-lying

excitations with positive parity or with angular momentum different from unity may not decay by electric-dipole emission of an *M* x ray. In particular, the lowest singly excited $3d \rightarrow 4s$ excitation may decay only via electric-quadrupole emission. The radiative lifetime of this excitation for Z near 53 is in the nanosecond range. To some extent, the metastability of this simple excitation is maintained even in the presence of additional $4s$ or $4p$ spectators in the *M* shell, giving rise to metastable states in the CuI and ZnI sequences. We note that even for these sequences, at high Z , autoionization of the lowest states with *M*-shell vacancies is not energetically allowed. This is to be contrasted to the situation generally confronting a system with a *K* or *L* vacancy and a small number of valence electrons, for which metastability is achieved only if selection rules hinder electron decay as well as radiative decays.

Since the compilation of Moore,¹ the NiI isoelectronic sequence has been studied up to $Z = 42$ by Alexander *et al.*² and for $Z = 62, 64,$ and 66 by Burkhalter *et al.*³ Only electric-dipole decays were observed. Measurement of transition energies for $3d^9 4f \rightarrow 3d^{10}$ and $3d^9 4p \rightarrow 3d^{10}$ lines as high as $Z = 66$ allows one to construct formulas for interpolating with rather good confidence to energies in the NiI sequence for intermediate Z . No equivalent information appears to be available for the $3d^9 4s \rightarrow 3d^{10}$ quadrupole decays for Z above 33.¹ One is thus forced to rely on theoretical transition energies in interpreting the observed spectra, and the assessment of the accuracy of such calculations is a goal of this work.

II. EXPERIMENTAL ARRANGEMENT

Iodine beams ranging in energy from 40 to 62 MeV were excited in passage through $40\text{-}\mu\text{g}/\text{cm}^2$

carbon foils. Radiation from the beam was dispersed in a bent-crystal x-ray spectrometer and detected by a thin-window (5000-Å paralyne) flow proportional counter (see Fig. 1). With a 20-nA beam of I^{+9} incident on the foil, filling a beam spot approximately 2 mm in diameter, peak count rates of the order of 10 sec^{-1} were obtained with the exciting foil just upstream of the spectrometer's field of view. Because the spectrometer entrance slit extends parallel to the beam, a beam segment approximately 1.5 cm in length was viewed at any foil position. This extended spatial resolution roughly matches the lifetimes studied, as described in Sec. IV, and will affect only the apparent relative component strengths if a multi-component decay curve is observed. Typical pressure in beam line and target area was several multiples of 10^{-6} Torr; excitation of the beam by residual gas was negligible. The spectrometer was stepped in uniform-wavelength increments upon collection of a present amount of integrated beam current. Distance between the foil and viewed region was varied by moving the foil without adjustment of the iodine beam optics. Calibration of the experimental energy scale was done using hydrogenic and heliumlike lines, whose energies are accurately known,⁴ from a foil-excited fluorine beam. Experimental transition energies listed in Table I are believed accurate to ± 0.5 eV for unblended lines.

III. GENERAL FEATURES OF SPECTRA

In Fig. 2, we show M x-ray spectra from iodine with the viewing area centered directly at the foil and at several downstream positions. The prompt spectrum displays lines so closely spaced that our resolution is inadequate to reveal much more

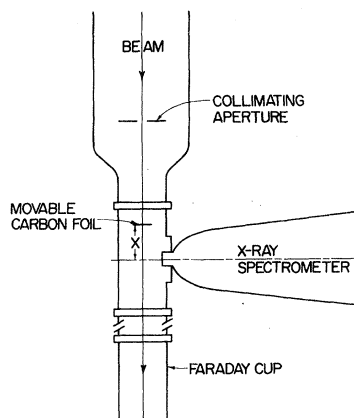


FIG. 1. Schematic of apparatus.

than the gross features of the spectrum. Areas of the spectrum in which one expects $4f \rightarrow 3d$, $4p \rightarrow 3d$, and $4s \rightarrow 3d$ transitions are indicated. These transition energies were calculated using the nonrelativistic Hartree-Fock program of Froese-Fischer.⁵ The strong rise in intensity at high energies is not fully understood but may be due in part to reflection into the proportional counter of far ultraviolet radiation.

The downstream spectra are considerably simplified. As expected, the great bulk of the emitting states have lifetimes too short to proceed beyond the foil, and the $4s \rightarrow 3d$ quadrupole transitions now dominate the spectrum. It is interesting that the $4p \rightarrow 3d$ region, though considerably weakened downstream, remains active. As discussed below, allowed $4p \rightarrow 3d$ transitions are much too fast for the emitting states to live for the nanosecond flight time between excitation and observation. It is possible that the presence of these lines downstream is due to their being cascade fed through longer-lived systems at higher excitation.

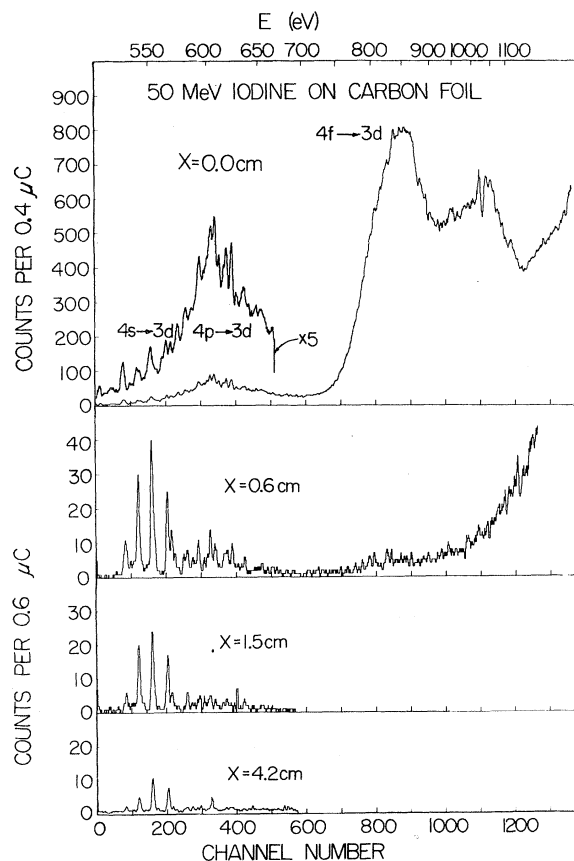


FIG. 2. Iodine M x-ray spectra taken at several different mean foil-detector distances x .

TABLE I. Transition energies in eV.

Initial	Final	E (NRHF)	Theory		E (RHF)	E _{exp}	(gf) ^b
			ΔE_R	E_T ^a			
Electric dipole transitions							
$3d^9(^2D_{5/2})4p_{3/2}$	$3d^{10}$	633.5	-13.4	620.1	621.9	621	0.281
$3d^9(^2D_{3/2})4p_{3/2}$	$3d^{10}$	645.4	-13.4	632.0	633.4	634	0.038
$3d^9(^2D_{3/2})4p_{1/2}$	$3d^{10}$	631.6	-13.4	618.2	616.8	616	0.048
$3d^9(^2D_{5/2})4s4p_{3/2}$	$3d^{10}4s$	621.3	-17.8	603.5	605.9	606	0.194
					605.4		0.195
					617.6		0.197
$3d^9(^2D_{3/2})4s4p_{3/2}$	$3d^{10}4s$	633.2	-17.8	615.4	614.3	616	0.008
					628.6		0.043
					615.9		0.011
$3d^9(^2D_{3/2})4s4p_{1/2}$	$3d^{10}4s$	619.4	-17.8	601.6	603.2	602	0.002
					599.1		0.020
					602.1		0.055
$3d^9(^2D_{5/2})4s^24p_{3/2}$	$3d^{10}4s^2$	609.4	-13.5	595.9	597.3	591	0.292
					607.8		0.037
$3d^9(^2D_{3/2})4s^24p_{3/2}$	$3d^{10}4s^2$	621.3	-13.5	607.8	608.6		0.037
$3d^9(^2D_{3/2})4s^24p_{1/2}$	$3d^{10}4s^2$	607.4	-13.5	593.9	592.9	587	0.037
Electric quadrupole transitions							
							(gf × 1000) ^b
$3d^9(^2D_{3/2})4s$	$3d^{10}$	592.5	-26.8	565.7	565.1	565.3	0.064
$3d^9(^2D_{5/2})4s$	$3d^{10}$	580.7	-26.8	553.9	552.8	552.9	0.073
$3d^9(^2D_{3/2})4s^2$	$3d^{10}4s$	584.7	-31.2	553.5	555.2	555	0.052
$3d^9(^2D_{5/2})4s^2$	$3d^{10}4s$	572.9	-31.2	541.7	542.7	543	0.079
$3d^9(^2D_{3/2})4s^24p$	$3d^{10}4s4p$	572.9	-26.1	546.8	547.4	543	0.027
					522.5		0.042
					535.9		0.020
					534.4		0.047
					545.5		0.013
					549.7		0.042
548.1	0.038						
$3d^9(^2D_{5/2})4s^24p$	$3d^{10}4s4p$	561.1	-26.1	535.0	534.9	533	0.038
					531.9		0.025
					544.4		0.037
					532.7		0.081
					523.8		0.032
					536.3		0.021
537.6	0.052						
534.8	0.116						

^a The sum of columns 3 and 4.^b From the RHF calculations.

Such persistence in the beam of short-lived states far from the excitation point has been previously observed in fluorine and oxygen,⁹ where the feeding states were believed to owe their long lifetimes to having one electron in a shell characterized by very high principal quantum number. If such a process is responsible for our observation

of $4p \rightarrow 3d$ transitions at large foil-detector distances, however, the apparent simplification of this region of the spectrum downstream is not immediately explained. One would expect a cascading network not to be particularly selective in its choice of states to be fed, whereas the observations show that the large "background" in

the $4p \rightarrow 3d$ region appears to die more rapidly with foil-detector distance than do selected lines.

An alternative reason for the persistence of lines in the $4p \rightarrow 3d$ region is that states whose angular-momentum quantum numbers forbid their electric-dipole decay may have intrinsically long lifetimes. Their emission of M x rays downstream might proceed via magnetic-quadrupole radiation or through electric-dipole radiation induced by hyperfine mixing. Unfortunately, our resolution in this region of the spectrum does not appear to be adequate to allow us to resolve this question of the basis of line identifications.

IV. LINE IDENTIFICATIONS

A. Excitation functions

In the absence of sufficient information to reliably predict the $4s \rightarrow 3d$ transition energies from trends along the isoelectronic series, we have been forced to rely on calculated transition energies to identify the observed lines. The relatively clean lines at 533, 543, 553, and 565 eV, hereafter referred to as peaks 1, 2, 3, and 4, respectively (see Fig. 3), are believed to be transitions of this type. Since the nonrelativistic calculations which we had in hand at the beginning of this work were not sufficiently accurate to identify unambiguously even the ionization levels of the emitting systems, we sought additional experimental clues to the identity of the emitting species from the excitation functions of the strongest lines.

Equilibrium charge fractions of iodine beams emerging from carbon foils in our energy range are known from the work of Moak *et al.*⁷ If the excitation distribution within an ionization state is not sensitively dependent upon the beam energy, the energy dependence of the x-ray yield from an excited state will be governed by the fraction of its parent charge state present in the post-foil beam. While the assumption of a constant excitation distribution is not automatically valid, it has been found to be sufficiently so in numerous cases to allow the use of this method to identify charge states of emitting species.

In Fig. 4 we compare the excitation functions for peaks 2-4 with charge-state equilibrium curves taken from Ref. 7. Both x-ray yields have been corrected for the velocity-dependent fraction of decay length viewed. This analysis suggests that peaks 2-4 are to be predominantly associated with charge states 24^+ and 25^+ , CuI and NiI sequences. This interpretation is consistent with that developed later on the basis of accurate transition-energy calculations. Our inability to pursue the excitation functions to higher-beam energy where the active charge states represent a larger frac-

tion of the beam prevents us from distinguishing between these two charge states. Indeed, peaks 2 and 3 probably contain contributions from more than one charge state.

B. Transition energies

The ultimate interpretation of the spectrum relies on having accurate theoretical transition energies. We compare our experimental energies with those obtained from two different calculations.

a. Nonrelativistic Hartree-Fock. In the first calculation, done at Kansas State University, the nonrelativistic Hartree-Fock (NRHF) program of Froese-Fischer⁵ was used without configuration mixing to compute adiabatic transition energies. In order to determine an appropriate coupling scheme, the spin-orbit Hamiltonian [$H = \sum_i (\xi \mathbf{l} \cdot \mathbf{s})_i$, where the sum is over valence electrons and ξ is defined by Ref. 8], was diagonalized for the states $(3d^9 4s)_j$ and $(3d^9 4p)_j$ in the Ni I sequence. The result was that the eigenenergies were very close to those obtained in pure jj coupling. We thus proceeded to compute energies for $4s \rightarrow 3d$ and $4p \rightarrow 3d$ transitions in the Ni I, Zn I, and Cu I sequences in jj coupling, using values of the param-

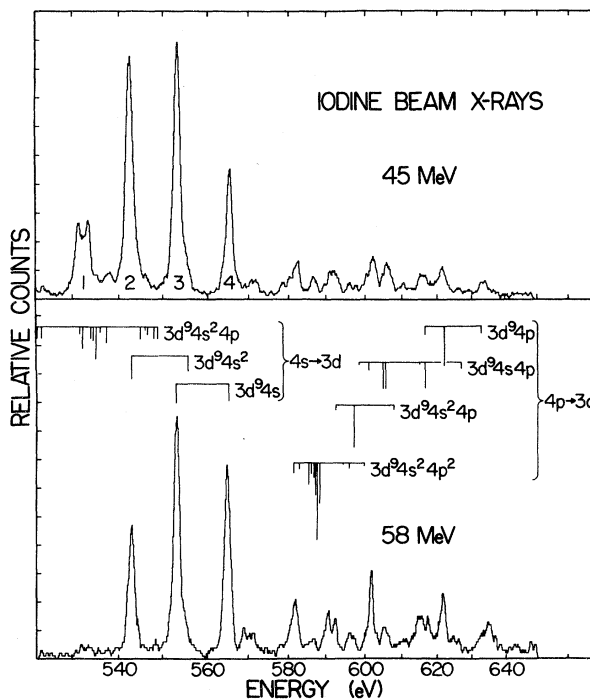


FIG. 3. Iodine M x-ray spectra taken with the foil just upstream of the viewed region. The calculated RHF line positions are indicated by vertical lines whose heights are proportional to the calculated gf values.

eters ξ computed by the NRHF program. The results are shown in column 3 of Table I.

These values display no agreement with the observed energies shown in column 7 of Table I. Suspecting that the reason for the discrepancy might be that relativistic terms in the Hamiltonian are important, we evaluated diagonal matrix elements of the "mass-velocity" and "Darwin" Hamiltonians $\{H_m = -\frac{1}{4}\alpha^2[E^0 - V(r)]^2$ and $H_d = -\frac{1}{4}\alpha^2[(dV/dr)](d/dr)$, respectively; see Ref. 9} using the Hermann-Skillman self-consistent-field program,⁹ as modified by Bhalla *et al.*¹⁰ These contributions, denoted by ΔE_R , were found to be quite large and are listed in column 4 of Table I. The corresponding corrected transition energies, the sum of columns 3 and 4, are shown in column 5 and are seen to be in good agreement with the observed energies. We remark that ΔE_R contains important contributions from the inner shells as well as valence electrons.

b. Relativistic Hartree-Fock. The second calculation, done at Lawrence Livermore Laboratories (hereafter denoted as RHF), was to use a Hartree-Fock average-configuration program to generate a set of basis functions which were then used to diagonalize a relativistic Hamiltonian. The basis states consisted of all of the states with a given j of the major configuration and those of one or two additional low-lying configurations of the same purity. This approach yielded excellent agreement between experiment and theory for the Ni I and Cu I isoelectronic series, lying within the experimental bars for these cases.

C. Spectral Interpretation

With the help of these calculations we can give a more detailed interpretation of our spectra (Fig. 3).

1. Electric-quadrupole transitions

The only unblended spectral line in the region between 530 and 570 eV we believe to be peak 4. This line is identified as the $[(3d^9)_{5/2}(4s)_{1/2}]_{J=2} \rightarrow (3d^{10})_{J=0}$ transition, and is the highest-energy $3d \rightarrow 4s$ transition. This identification is supported by agreement between experimental and calculated transition energies, the excitation function for the line, and the observation that no strong isolated lines appear at higher energies in this section of the spectrum.

Other apparently clean lines in this region are in fact blends. Peak 3 should contain contributions for both $[(3d^9)_{3/2}(4s_{1/2})]_{J=2} \rightarrow (3d^{10})_{J=0}$ and $(3d^9)_{5/2}(4s_{1/2})^2 \rightarrow (3d^{10}4s_{1/2})$, whose sum explains the greater intensity of this line relative to that of peak 4. The high-energy shoulder on this peak

is probably due to the latter transition. At the higher-beam energies this contribution becomes relatively weaker, since it represents the lower-charge state. Similarly, peak 2 may contain contributions from decays from $(3d^9)(4s_{1/2})^2$ and $3d^9 4s^2 4p$ configurations. The calculated spectrum from the latter configuration is quite rich in lines, and identifications of even the strongest of these lines in our spectrum do not seem to be unambiguous. We believe the doublet structure of peak 1 to originate from this configuration. That this peak belongs to a lower charge state is confirmed by its weakness at higher iodine energy.

2. Electric-dipole transitions

Three lines from the $(3d_{j_1}^9 4p_{j_2})_{J=1} \rightarrow 3d^{10}$ transition with $(j_1, j_2) = (\frac{3}{2}, \frac{1}{2}), (\frac{5}{2}, \frac{3}{2}),$ and $(\frac{3}{2}, \frac{3}{2})$ are observed at 616, 621, and 633 eV, respectively. The delayed spectrum shows no spectral lines above 633 eV, an observation which supports our identification of this line. It is the highest-energy $4p \rightarrow 3d$ transition possible with a single vacancy in the $3d$ shell. Lines originating from

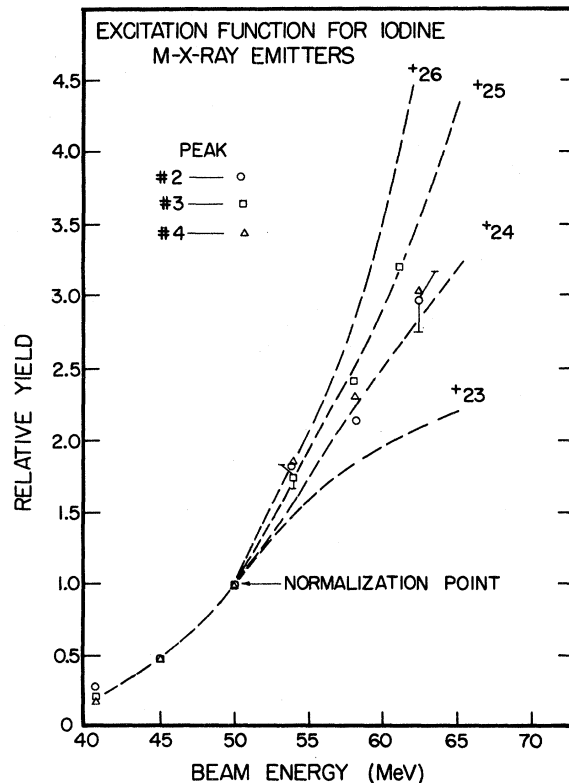


FIG. 4. Excitation functions for peaks 2-4 (see text and Fig. 3) are shown as data points. Charge-state equilibrium curves from Moak *et al.*, Ref. 7, are shown as dashed lines. Both x-ray yields and charge-state curves are normalized to unity at 50 MeV.

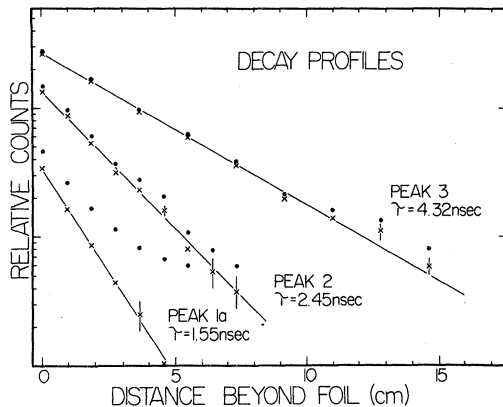


FIG. 5. Decay profiles for peaks 1a, 2, and 3, corresponding to x-ray energies of 532, 543, and 553 eV, respectively. The raw data are shown as filled circles. After subtraction of the background, as described in the text, the x 's remain.

the $3d^9 4s4p$ and $3d^9 4s^2 4p$ configurations are tentatively identified with features on the spectrum in Table I, but the spectrum is too complex for unambiguous interpretation. Indeed, if these lines originate from states whose $E1$ decay is not allowed, comparison of observed energies with those calculated for allowed $E1$ decays is not particularly meaningful. The $(3d^9 4p) \rightarrow 3d^{10}$ transition energy of 633 eV is in fair agreement with the value of 631 eV obtained from the formula given by Burkhalter *et al.*³

V. LIFETIMES

Decay profiles were taken for peaks 1–4, of which examples are shown in Fig. 5. Since a small background under the peaks was apparent from the spectra, background decay profiles were taken at wavelengths adjacent to each peak and were subtracted from the profile centered on the peak. The background was quite significant for peaks 1a and 1b, centered at 531 and 533 eV, respectively, and less so for peaks 2–4. The remaining decay curves were observed to be nearly

single exponential in form, and the quoted lifetimes in Table II were deduced assuming such a shape.

The major contributor to the quoted error is uncertainty associated with assignment of cascade or background contributions. Peak 4 showed a major decay with a lifetime of 4.1 ± 0.2 nsec. Since this is presumably a single line, we compare, in Table II, this experimental value with the lifetime calculated for the $(3d^9 4s)_{5/2} \rightarrow 3d^{10}$ electric-quadrupole transition. The major decay component in peak 3 gave a lifetime of 4.3 ± 0.1 nsec. While this peak is a blend of $(3d^9 4s)_{3/2} \rightarrow 3d^{10}$ and $(3d^9 4s^2)_{5/2} \rightarrow 3d^{10} 4s$ transitions, the measured lifetimes for these transitions are quite similar. However, we point out that, for the CuI and higher sequences, the $E2$ decay is not the only open radiative channel. For example, the $3d^9 4s^2$ configuration lies above the $3d^{10} 4p$ configuration, and mixing of the initial state with the $3d^9 4p^2$ configuration allows its decay via an electric-dipole photon. As one adds $4p$ electrons, competition between electric-quadrupole and electric-dipole decays should become more important, and thus comparisons between observed decay slopes and calculated $E2$ rates may cease to be meaningful. Peaks 1 and 2 both display shorter-lived major components than could be explained on the basis of $E2$ decay alone, thus supporting the contention that $E1$ decays are becoming important. The more rapid decay of peak 2, relative to that of peak 3, may be attributed to $3d^9 4s^2 - 3d^9 4p^2$ mixing, which has shortened the lifetime of the $3d^9 4s^2$ state, or to the presence in peak 2 of appreciable strength from initial states of the $3d^9 4s^2 4p$ configuration. The nearly single-exponential character of the decay favors the former interpretation. In this case, one might expect a shorter-lived component to appear in the decay profile for peak 3 as well. However, since the decay curve for this peak was taken slightly to the low-energy side of the peak, it is likely that the decay profile of peak 3 is dominated by the

TABLE II. Lifetimes (τ) in nsec.

Initial	Final	Calculated		Peak	Observed	τ
		τ ($E2$ only)				
		NRHF	RHF		Energy (eV)	
$3d^9(^2D_{3/2})4s$	$3d^{10}$	5.93	5.606	4	565	4.11 ± 0.1
$3d^9(^2D_{5/2})4s$	$3d^{10}$	5.80	5.15	3	553	4.38 ± 0.1
$3d^9(^2D_{3/2})4s^2$	$3d^{10}$	6.05	5.70			
$3d^9(^2D_{5/2})4s^2$	$3d^{10}$	6.74	5.93	2	543	2.52 ± 0.1
				1a	532	1.55 ± 0.2
				1b	534	2.85 ± 0.2

$(3d^9 4s)_{3/2} \rightarrow 3d^{10}$ transition.

In Table II we compare observed decay times with calculated $E2$ lifetimes. The NRHF values were calculated using intermediate-coupling wave functions, since transition rates are more sensitive to departures from jj coupling than are the transition energies. The RHF decay times were calculated using matrix elements for the calculated eigenstates of the velocity-type forms of the transition operator. The observed lifetime of 4.1 ± 0.2 nsec for the $(3d^9 4s)_{5/2} \rightarrow 3d^{10}$ decay, whose interpretation appears unambiguous, is somewhat shorter than the theoretical ones. We note that the presence of undetected long-lived cascades in the decay curve would have led to our extracting a lifetime erroneously too long, not too short.

VI. CONCLUSIONS

The present experiment demonstrates the usefulness of foil-excited high-energy ion beams in

expanding our knowledge of the spectra of very highly ionized systems whose radiative decay is in the soft x-ray region. Electric-dipole-forbidden decays are particularly easy to study using this radiation source, and their radiative lifetimes may be measured. However, allowed decays do appear in the spectra as well, and their transition energies can be measured. Hartree-Fock calculations of adiabatic transition energies were found to be in excellent agreement with observed transition energies, especially for nearly closed-shell configurations. However, contributions from relativistic parts of the Hamiltonian to the transition energies are quite important, even for the rather modest transition energies near 500 eV, in very highly ionized systems. One thus has some confidence that neighboring members of the Ni I, Cu I, and Zn I isoelectronic sequences will be handled rather well by similar calculations.

*Supported in part by the Office of Naval Research and by the Energy Research and Development Administration.

†Present address: Dunn & Bradstreet, Union, N. J.

‡Present address: Bell Laboratories, Murray Hill, N. J. 07974.

§Present address: Dresser Industries, Houston, Tex.

|| Present address: Los Alamos National Lab., Los Alamos, N. M. 87544.

¹Charlotte E. Moore, N.B.S. Circular No. 467, (U.S.G.P.O., Washington, D. C., 1952).

²E. Alexander, M. Even-Zohar, B. S. Fraenkel, and S. Goldsmith, *J. Opt. Soc. Am.* **61**, 508 (1971).

³P. G. Burkhalter, D. J. Nagel, and R. R. Whitlock, *Phys. Rev. A* **9**, 2331 (1974).

⁴R. L. Kauffman, C. W. Woods, F. F. Hopkins, D. O. Elliott, K. A. Jamison, and P. Richard, *J. Phys.* **B** **6**, 2197 (1973).

⁵C. Froese-Fischer, *Comp. Phys. Commun.* **4**, 107 (1972); **1**, 151 (1969).

⁶W. J. Braithwaite, D. L. Matthews, and C. F. Moore, *Phys. Rev. A* **11**, 465 (1975); P. Richard, *Phys. Lett.* **45A**, 13 (1973); P. Richard, R. L. Kauffman, F. F. Hopkins, C. W. Woods, and K. A. Jamison, *Phys. Rev. Lett.* **30**, 888 (1973), and *Phys. Rev. A* **8**, 2187 (1973).

⁷C. D. Moak, L. B. Bridwell, H. O. Lutz, S. Datz, and L. C. Northcliffe, *Beam-Foil Spectroscopy*, edited by S. Bashkin (Gordon and Breach, N. Y. 1968), p. 157.

⁸M. Blume and R. E. Watson, *Proc. R. Soc. A* **27**, 127 (1962).

⁹F. Hermann and S. Skillman, *Atomic Structure Calculations* (Prentice-Hall, Englewood Cliffs, N. J., 1963).

¹⁰C. P. Bhalla, N. O. Folland, and M. A. Hein, *Phys. Rev. A* **8**, 649 (1973).